FOOT@BO

Riccardo Ridolfi

on behalf of the FOOT Bologna team
Riccardo.Ridolfi@bo.infn.it

30 January 2023

Hadrontherapy

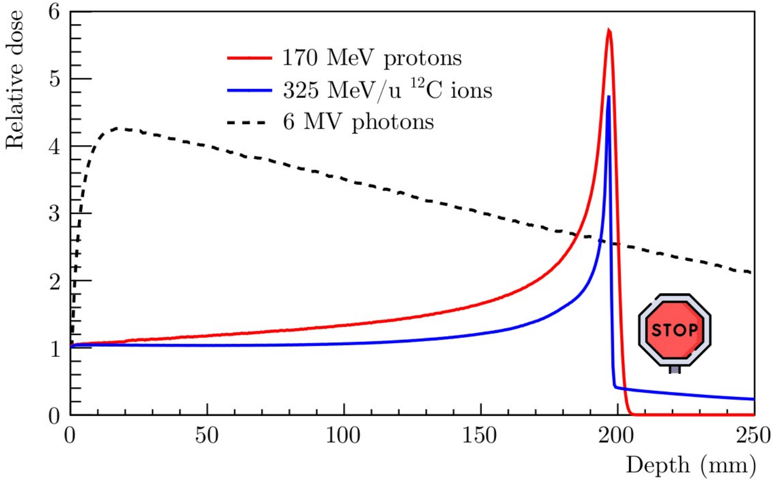

-**low dose** in the entrance channel
-**Bragg peak**
-**range** can be **adjusted** with
incident ion energy

Hadrontherapy

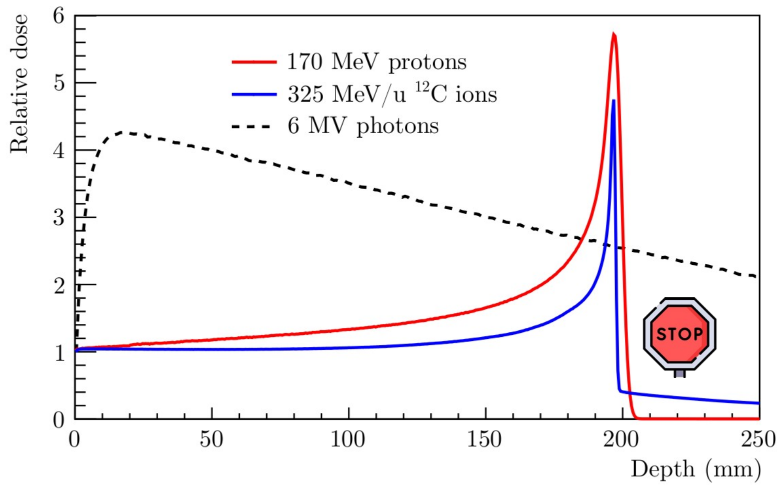

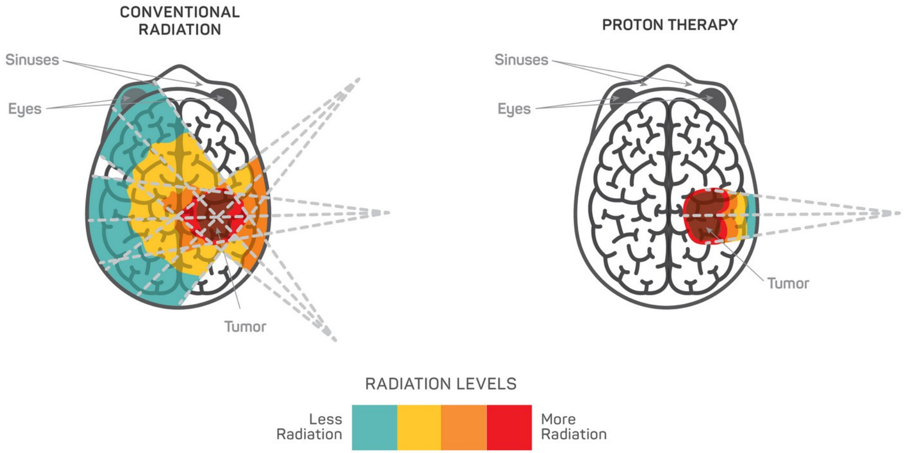

-**low dose** in the entrance channel
-**Bragg peak**
-**range** can be **adjusted** with incident ion energy
-powerful for treatment **near organs at risk**

Nuclear fragmentation

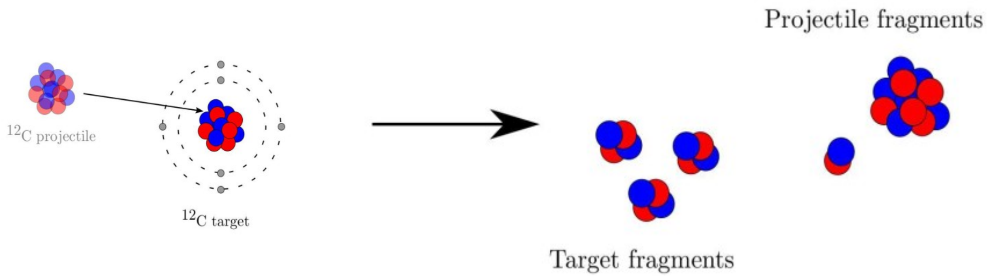

Nuclear fragmentation

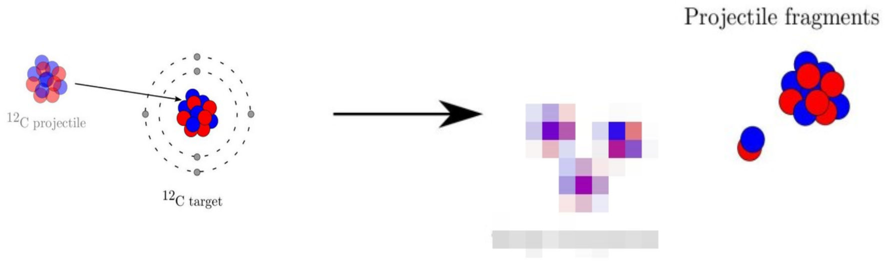

-projectile fragments have a **longer range**
-**non-zero dose** beyond the Bragg peak to address
-**not present** in protontherapy

Nuclear fragmentation

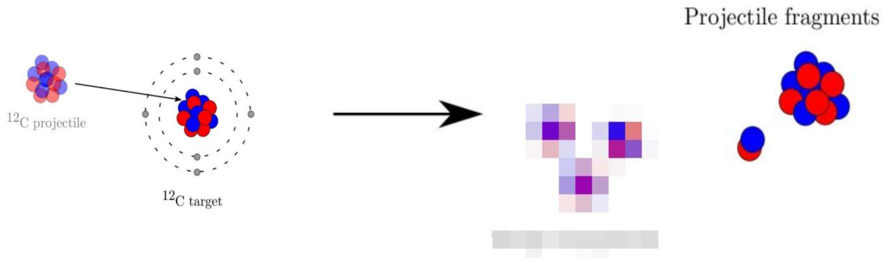

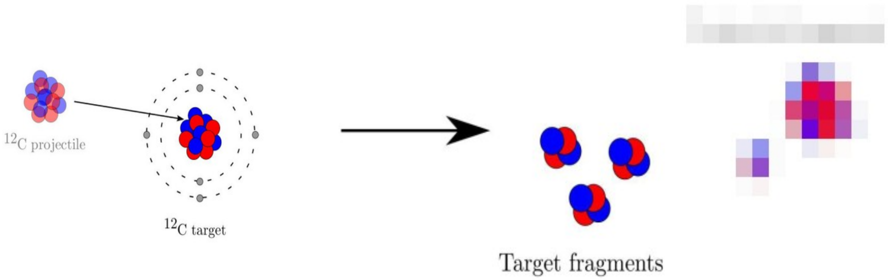

-projectile fragments have a **longer range**
-**non-zero dose** beyond the Bragg peak to address
-**not present** in protontherapy

-target fragments have very **low energies** (short range, hundreds of μm)
-**difficult to detect**
-their **damage** can be more important in **healthy tissues**
-biological **effectiveness of protons** still in question

Nuclear fragmentation

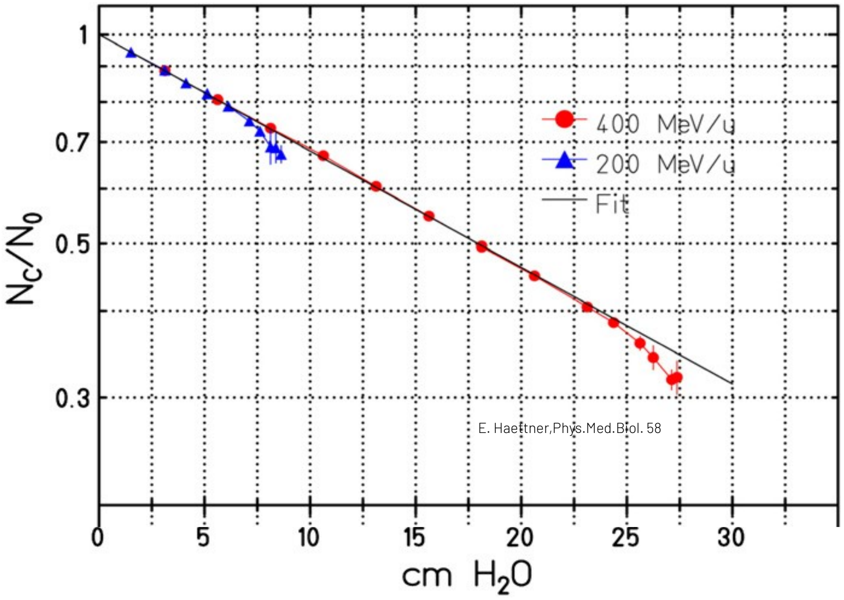

$$P(x) = \frac{N(x)}{N(0)} = \exp(-x/\lambda_{\rm int})$$

$$\lambda_{\rm int} = \frac{A_t}{N_a \sigma_R \rho}$$

-**attenuation** of primary beam can be important at **large** penetration **depths**
-**surviving ions** can be counted and **related to total reaction cross sections**

Nuclear fragmentation

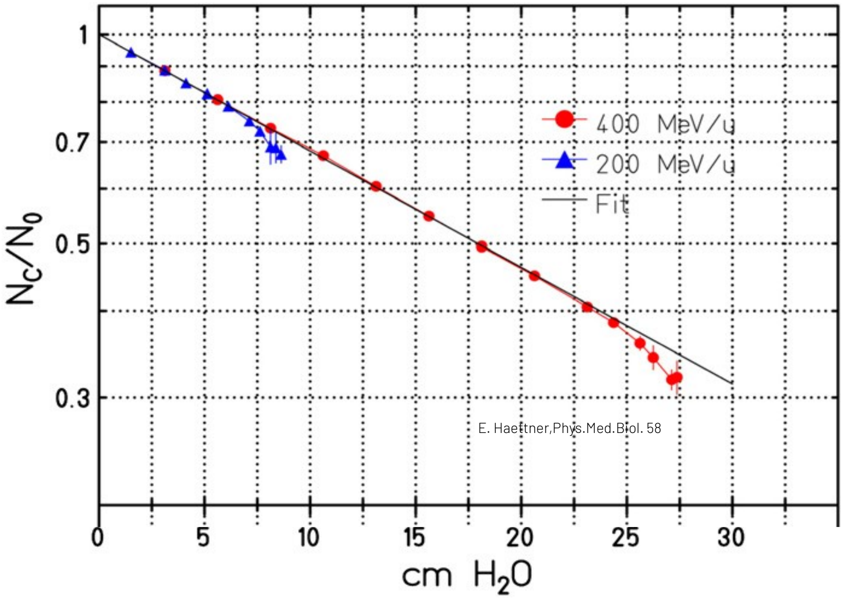

-**attenuation** of primary beam can be important at **large** penetration **depths**
-**surviving ions** can be counted and **related to total reaction cross sections**

$$P(x) = \frac{N(x)}{N(0)} = \exp(-x/\lambda_{\text{int}})$$

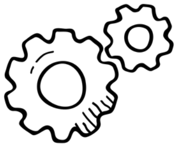

$$\sigma_R = \int_0^{\Omega}\int_0^{\infty} \frac{d^2\sigma}{dE_K d\Omega} dE_K d\Omega$$

$$\lambda_{\text{int}} = \frac{A_t}{N_a \sigma_R \rho}$$

Space radioprotection

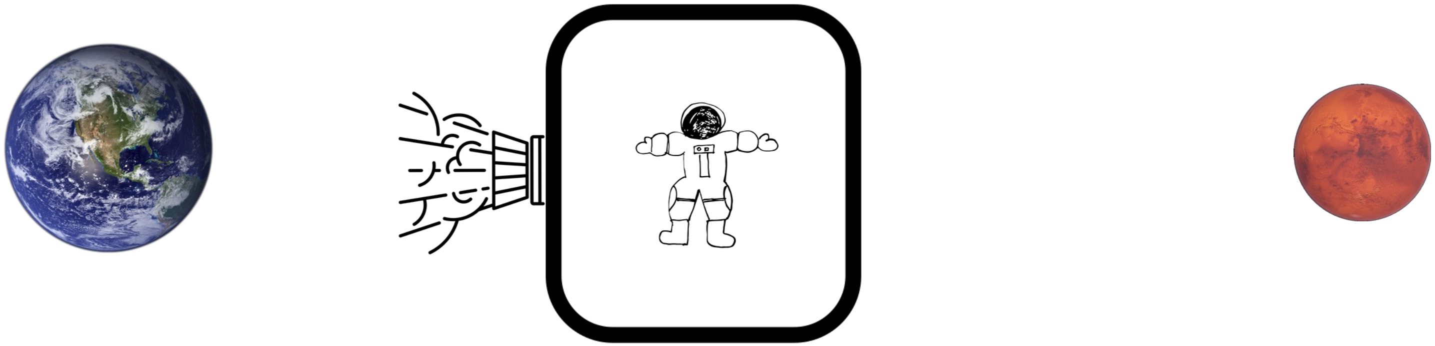

Space radioprotection

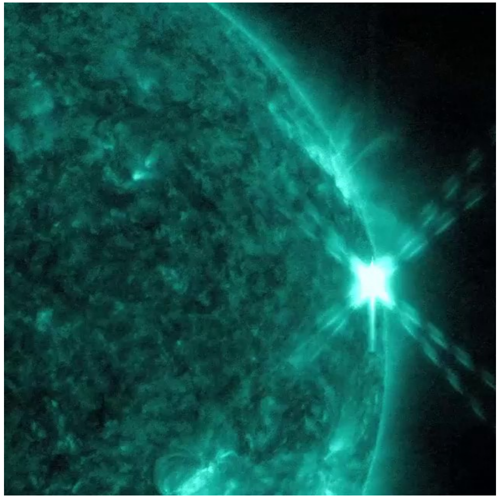

Solar Particle Events (SPEs)
suddenly
92% p
6% He
2% HZE

<1 GeV/n

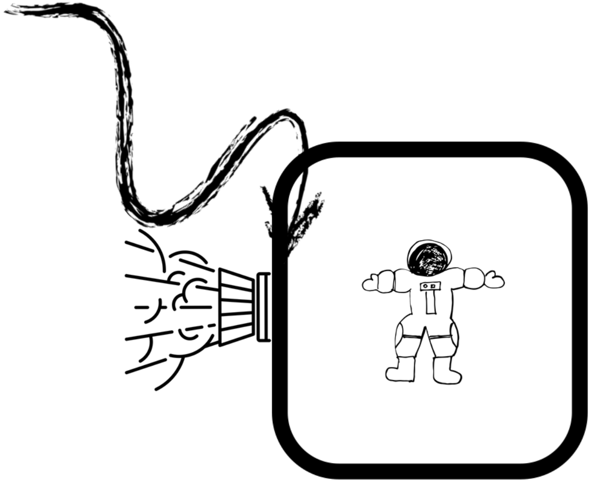

Space radioprotection

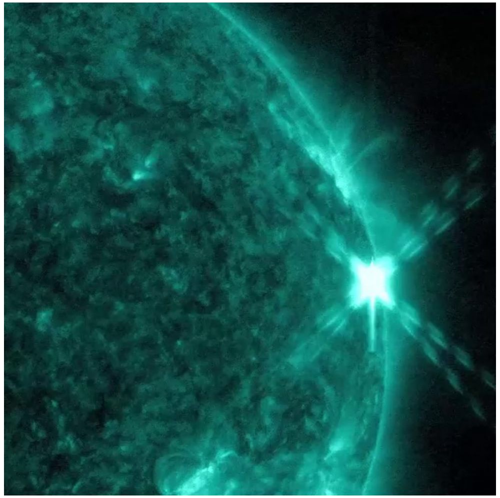

Solar Particle Events (SPEs)
suddenly
92% p
6% He
2% HZE

<1 GeV/n

Galactic Cosmic Rays (GCRs)
constantly
90% p
9% He
1% HZE

0.001-10^{14} GeV/n
(peak at 0.1-1 GeV/n)

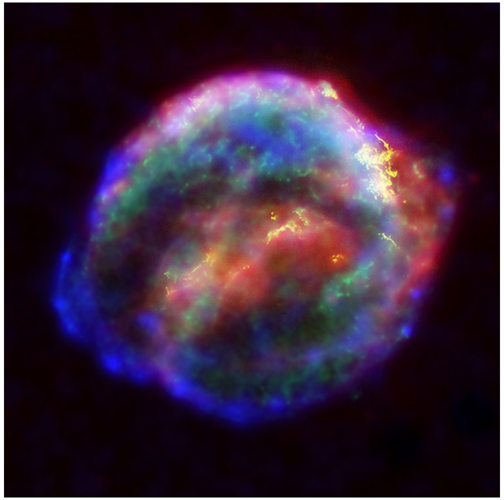

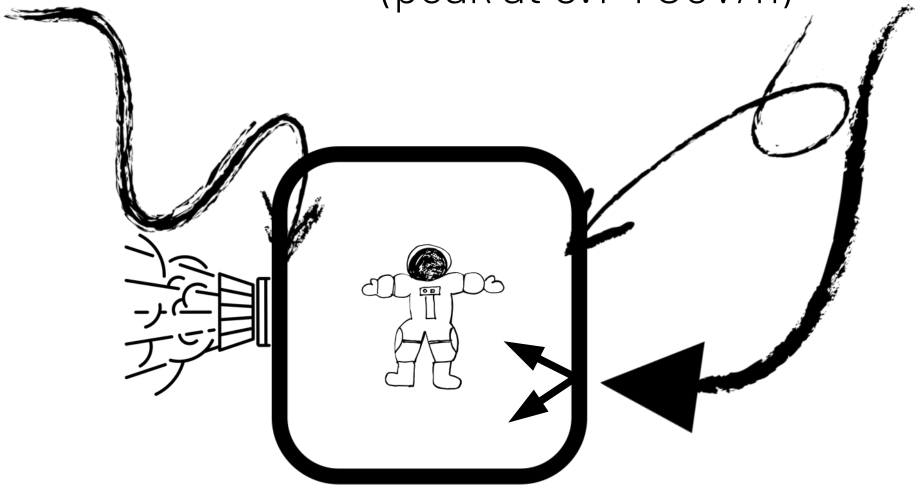

Space radioprotection

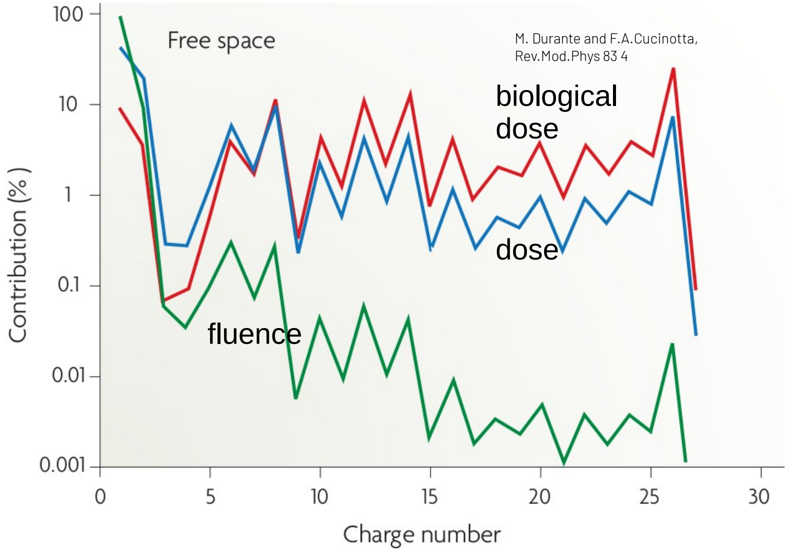

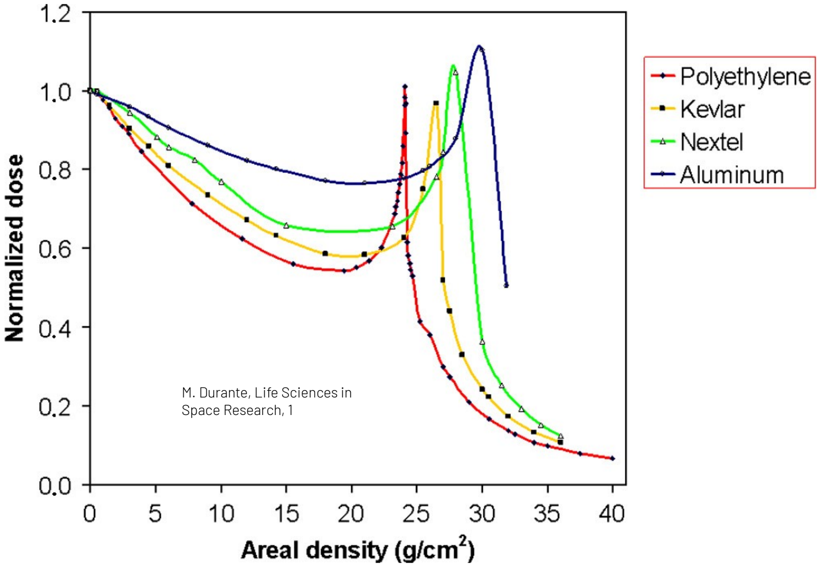

measurement of Bragg curves
in different materials of different
thicknesses

Space radioprotection

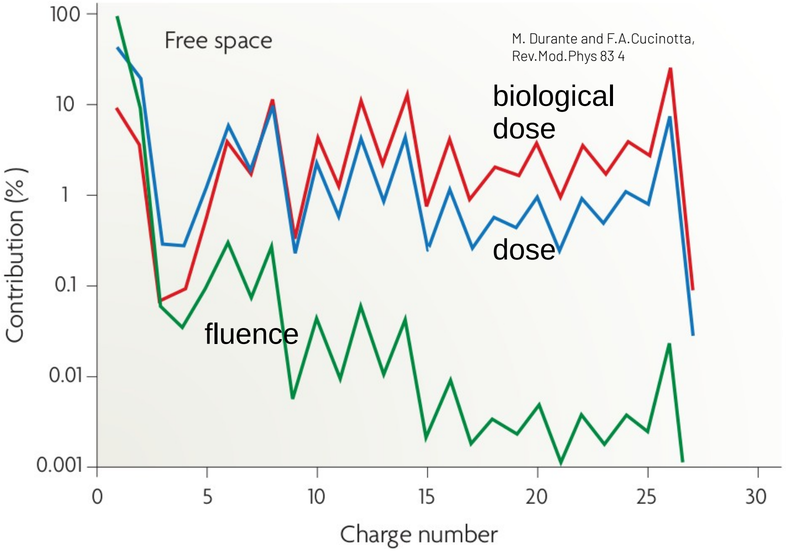

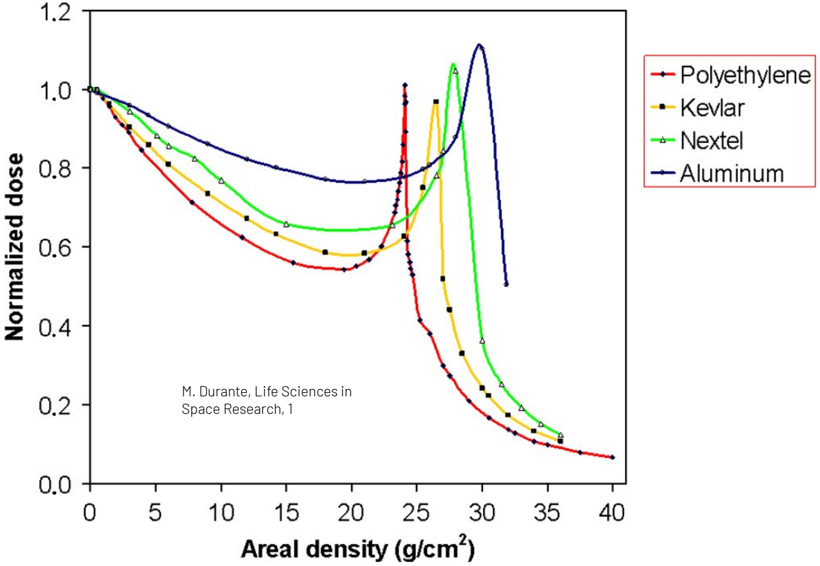

measurement of Bragg curves in different materials of different thicknesses

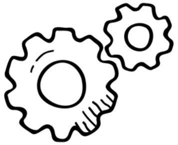

$$\sigma_R = \int_0^{\Omega} \int_0^{\infty} \frac{d^2\sigma}{dE_K d\Omega} dE_K d\Omega$$

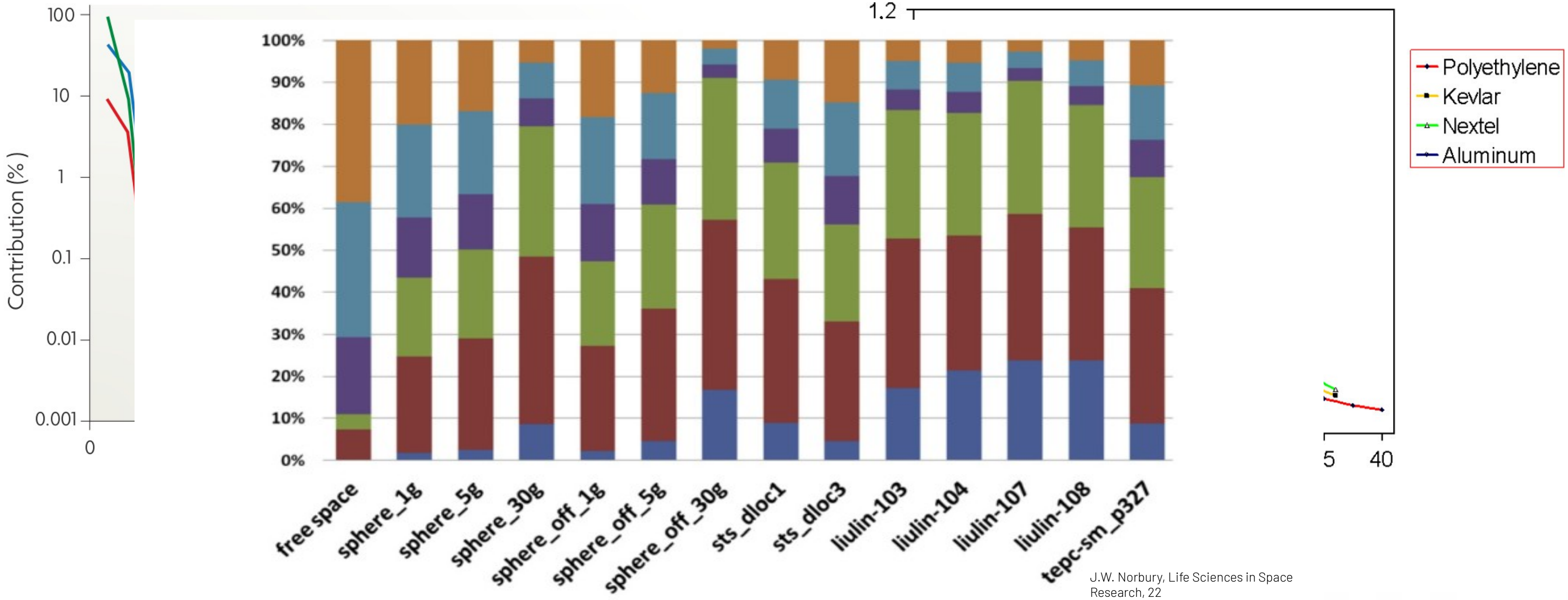

J.W. Norbury, Life Sciences in Space Research, 22

measure
in differe
thicknes

Fig. 22. Calculated percent contribution to blood forming organ (BFO) dose equivalent for free space (far left), simple spherical geometries in free space, and detector locations inside the space shuttle (STS) and the International Space Station (ISS) in free space. The vehicles included three aluminum spheres with areal densities 1, 5, and 30 g/cm^2 where the body was placed at the center of the sphere (sphere-1g, sphere-5g, sphere-30g) and three spheres of the same areal densities where the body was placed against the wall of the sphere (sphere- off-1g, sphere-off-5g, sphere-off-30g). For the latter cases, the spheres were constructed so that they would each have the same habitable volume as the Multi-Purpose Crew Vehicle (MPCV), 316 cubic feet (8.95 m^3) (NASA, 2011). Thus, each sphere had an inner radius of 1.288 m. In addition, six locations in the STS (shuttle) where detectors have historically been placed (sts-dloc1-6), for example see Benton and Benton (2001), were investigated. Five locations in the ISS 6A configuration were also used: two points in the Destiny (Lab) module laboratory area (Liulin-103, Liulin-107); two points in the Unity (Node1) module (Liulin-104, Liulin-108); and one point in the Zvezda (SM; service module) module on panel number 327 (TEPC-sm-p327). Reprinted from Walker et al. (2013) and Norbury and Slaba (2014).

$$\frac{\sigma}{d\Omega} dE_K d\Omega$$

The FOOT (FragmentatiOn Of Target) experiment

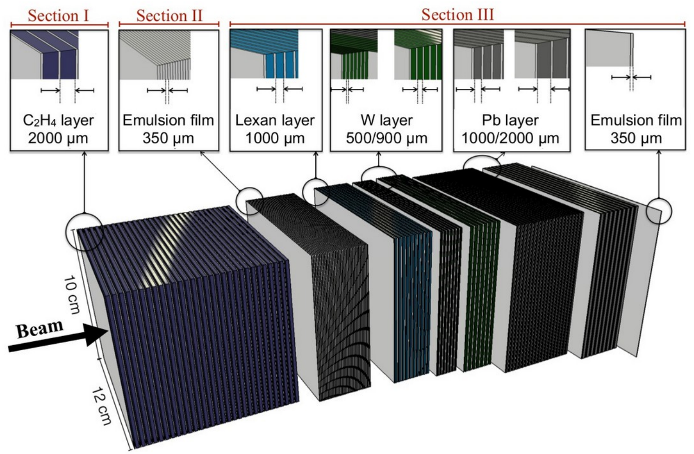

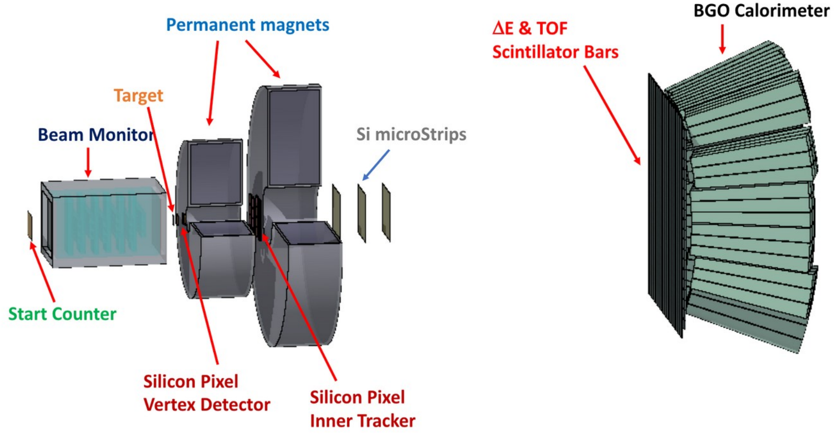

measurement of **double differential cross sections** in angle and kinetic energy with a maximum uncertainty of 5%

direct/inverse kinematics and cross section subtraction

isotopic identification by measuring all kinematic quantities

table top setup to be moved according to beam availability

the **core program** can be **extended** thanks to its flexibility

The FOOT experiment: core program

Physics	Application field	Beam	Target	Upper Energy (MeV/nucleon)	Kinematic approach
Target fragmentation	Hadrontherapy	^{12}C	C, C_2H_4	200	inverse
Target fragmentation		^{16}O	C, C_2H_4	200	inverse
Beam fragmentation	Hadrontherapy	^{4}He	C, C_2H_4, PMMA	250	direct
Beam fragmentation		^{12}C	C, C_2H_4, PMMA	400	direct
Beam fragmentation		^{16}O	C, C_2H_4, PMMA	500	direct
Beam fragmentation	Space	^{4}He	C, C_2H_4, PMMA	800	direct
Beam fragmentation		^{12}C	C, C_2H_4, PMMA	800	direct
Beam fragmentation		^{16}O	C, C_2H_4, PMMA	800	direct

The FOOT experiment: core program

Physics	Application field	Beam	Target	Upper Energy (MeV/nucleon)	Kinematic approach
Target fragmentation	Hadrontherapy	^{12}C	C, C_2H_4	200	inverse
Target fragmentation		^{16}O	C, C_2H_4	200	inverse
Beam fragmentation	Hadrontherapy	^{4}He	C, C_2H_4, PMMA	250	direct
Beam fragmentation		^{12}C	C, C_2H_4, PMMA	400	direct
Beam fragmentation		^{16}O	C, C_2H_4, PMMA	500	direct
Beam fragmentation	Space	^{4}He	C, C_2H_4, PMMA	800	direct
Beam fragmentation		^{12}C	C, C_2H_4, PMMA	800	direct
Beam fragmentation		^{16}O	C, C_2H_4, PMMA	800	direct

more beam-target settings **to explore...**

The FOOT experiment: emulsion setup

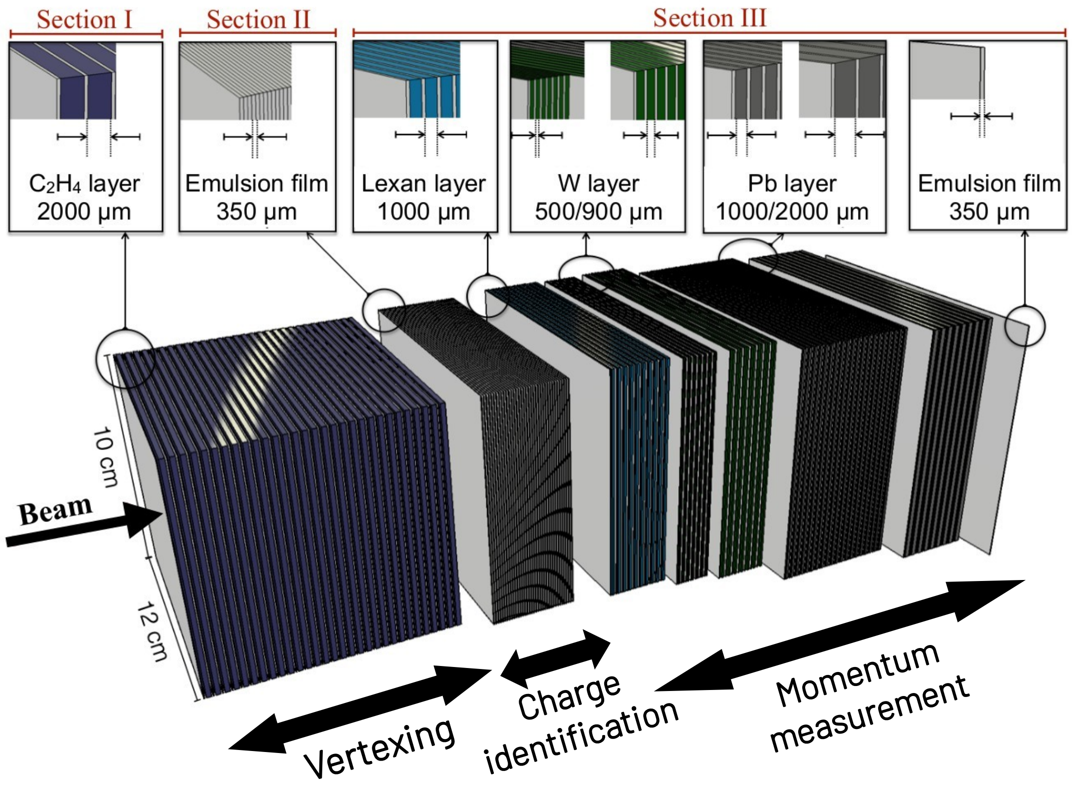

Emulsion Cloud Chamber setup

designed for **light fragments** ($Z \leq 3$)

high angular acceptance (70°)

no need of **real time data acquisition**

emulsions have to be **developed** after the irradiation

The FOOT experiment: electronic setup

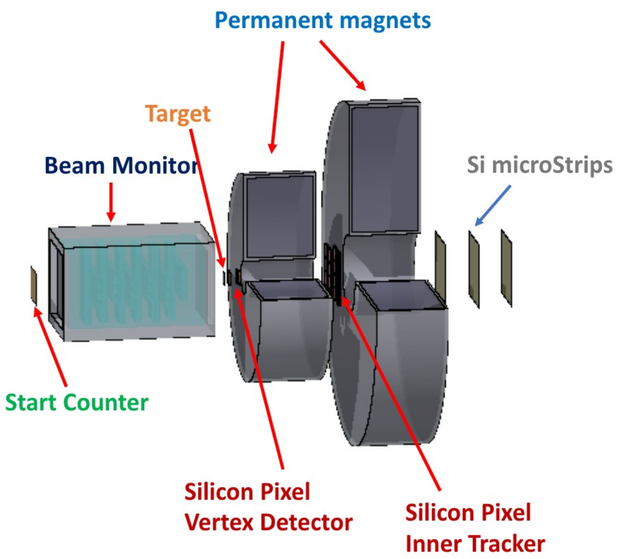

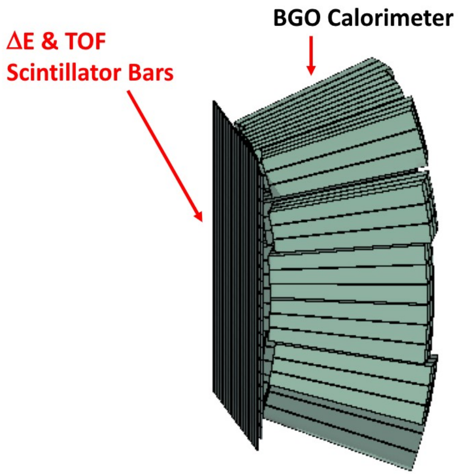

large variety of detectors

highly distributed data acquisition system

designed for **heavier fragments** ($3 \leq Z \leq 8$)

angular acceptance of **10°**

to be completed in **2023**

The FOOT experiment: electronic setup

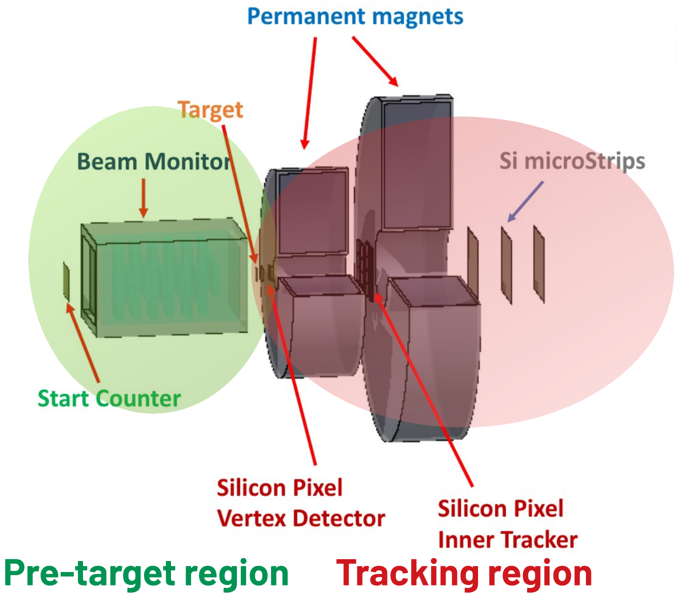

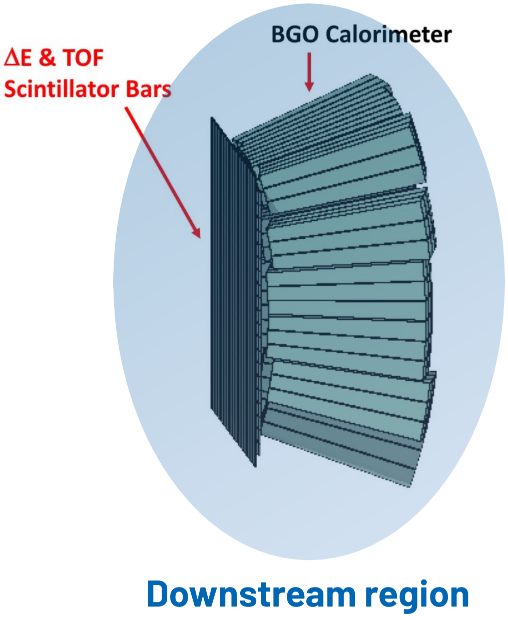

large variety of detectors

highly distributed data acquisition system

designed for **heavier fragments** ($3 \leq Z \leq 8$)

angular acceptance of **10°**

to be completed in **2023**

Electronic setup: pre-target region

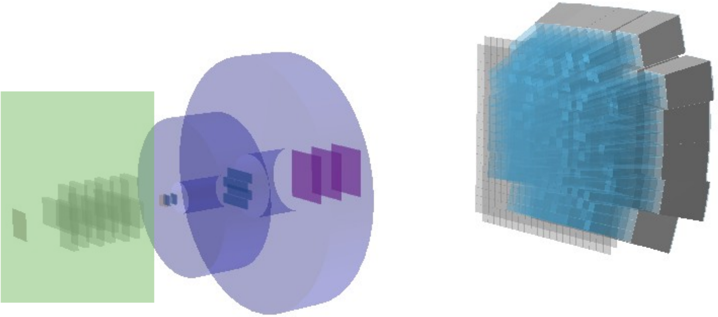

beam characterization

Start Counter (SC)

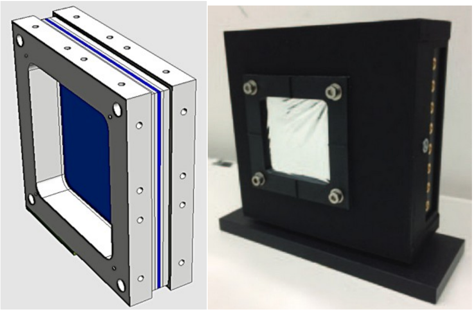

Trigger and ToF start

250 µm thick plastic scintillator

5x5 cm^2 active area

48 SiPM → 8 channels

Beam Monitor (BM)

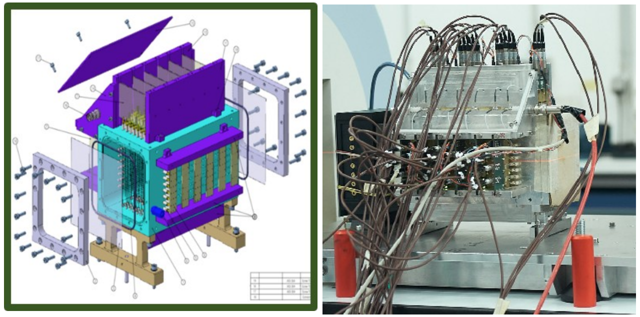

Beam momentum and direction

Rejection of pre-target fragmentation

Drift chamber Ar/CO_2 (80%/20%)

12 layers with 3 cells each (orthogonal views)

Electronic setup: tracking region

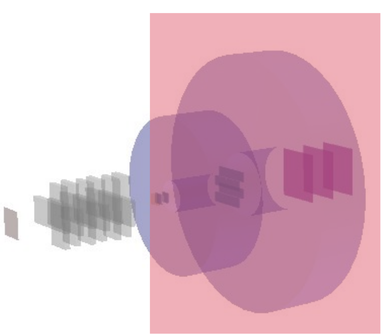

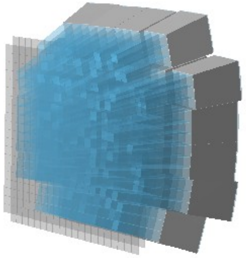

fragment tracking
momentum measurement

Vertex (VTX) &
Inner Tracker (IT)

Magnets

Microstrip detector
(MSD)

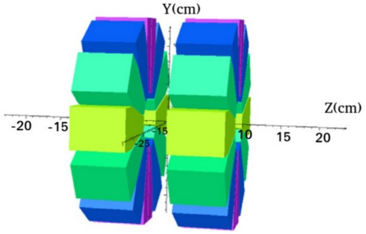

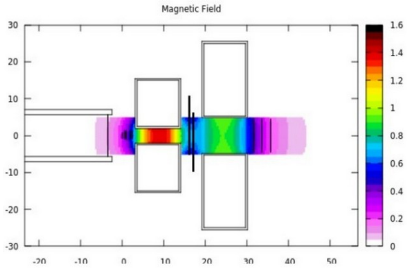

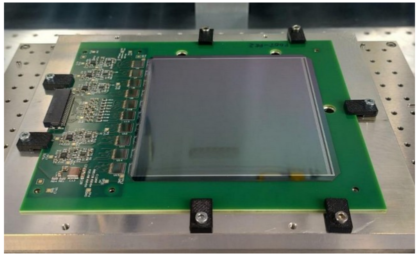

Mimosa-28 Si pixel
20 μm pitch
VTX→4 layers   IT→2 layers

2 permanent magnets Halbach
configuration
B field in y axis up to 1.2 T

3 pairs of X-Y layers
9 x 9 cm^2 active area
150 μm readout pitch

Electronic setup: downstream region

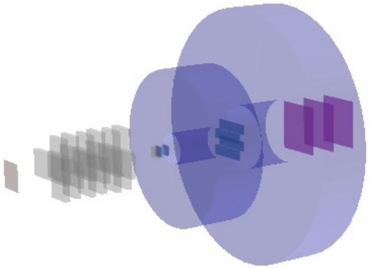

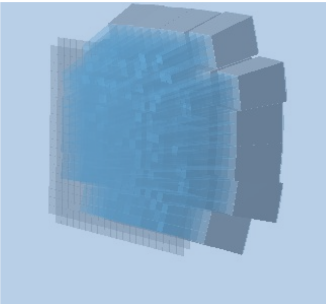

fragment identification

TOF Wall (TW)

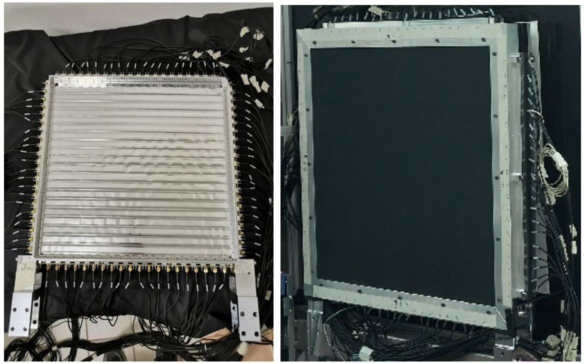

ΔE – TOF

44 cm x 2 cm x 3 mm plastic scintillator bars

2 layers of 20 bars each

SiPM readout

Calorimeter (CALO)

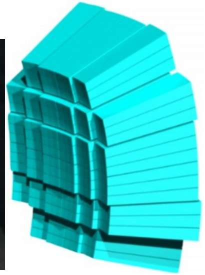

Kinetic energy

BGO scintillator

320 crystals 2 (3) x 2 (3) x 24 cm^3

Electronic setup: downstream region

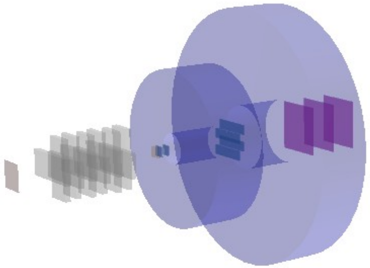

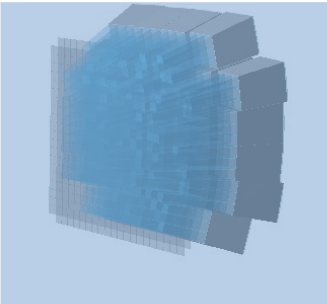

[fragment identification]

TOF Wall (TW)

Calorimeter (CALO)

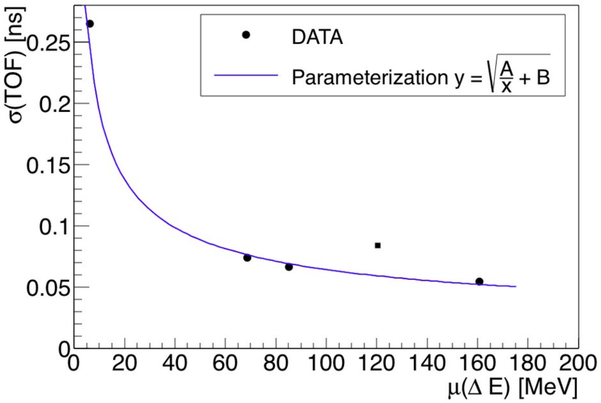

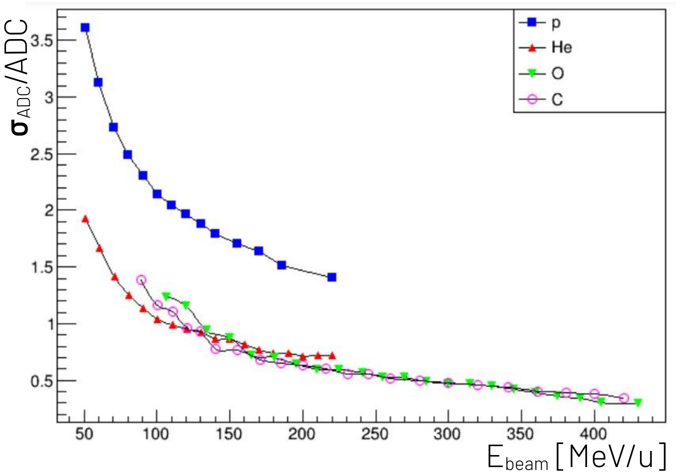

Data taking

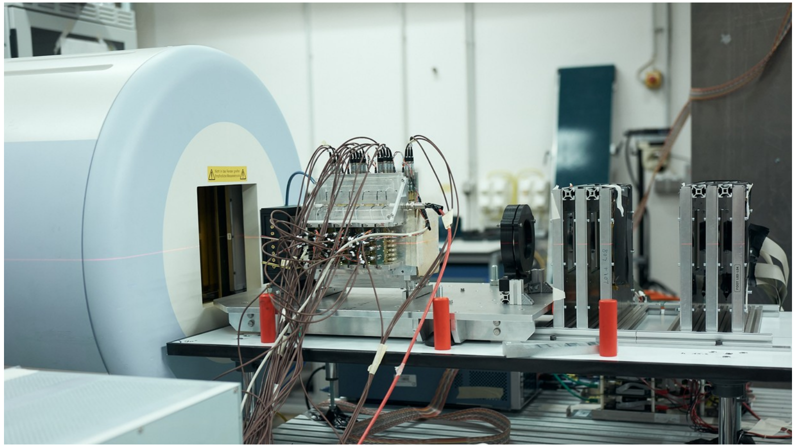

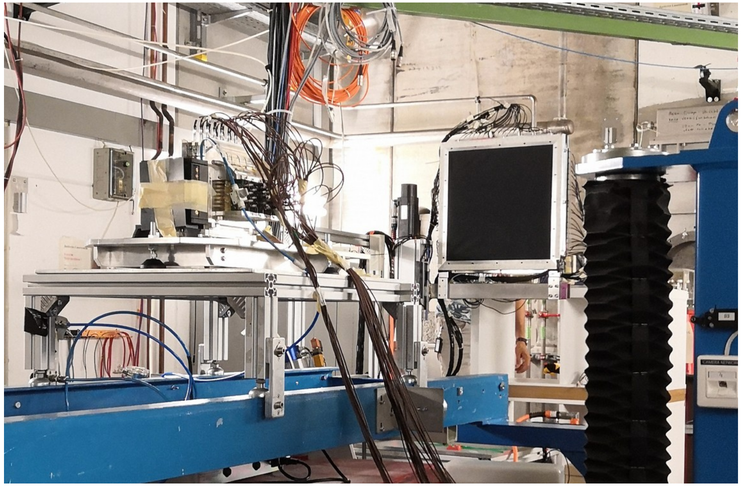

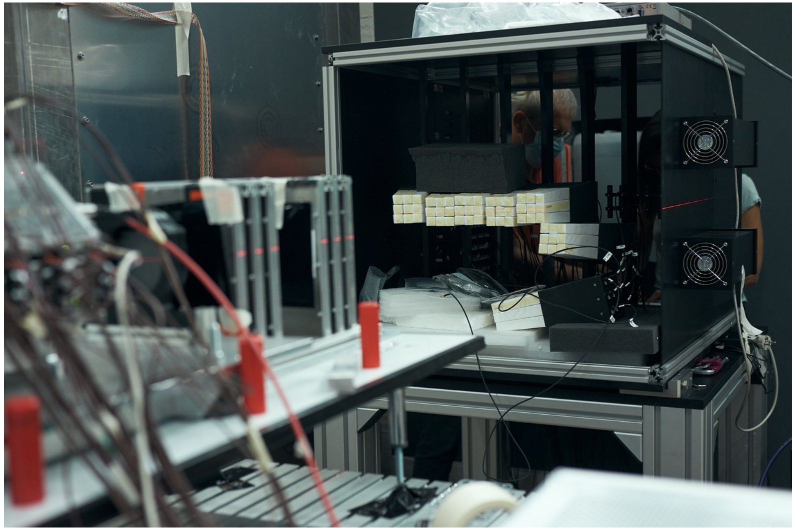

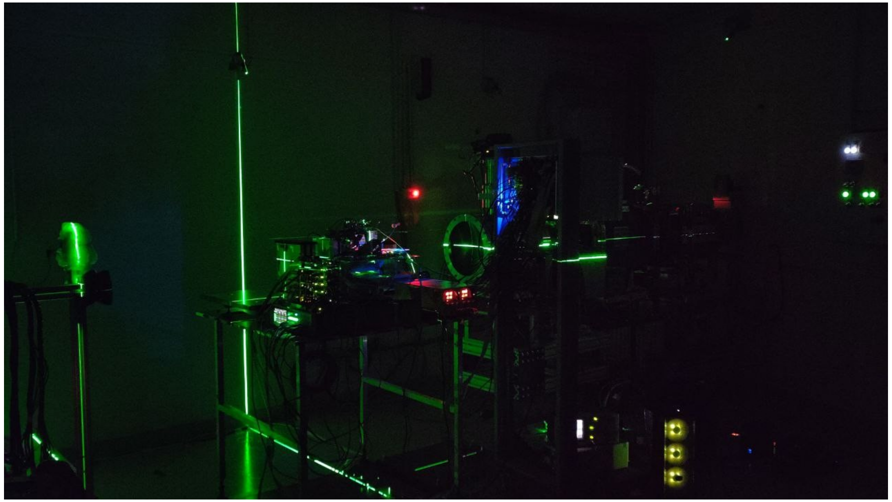

Data analysis

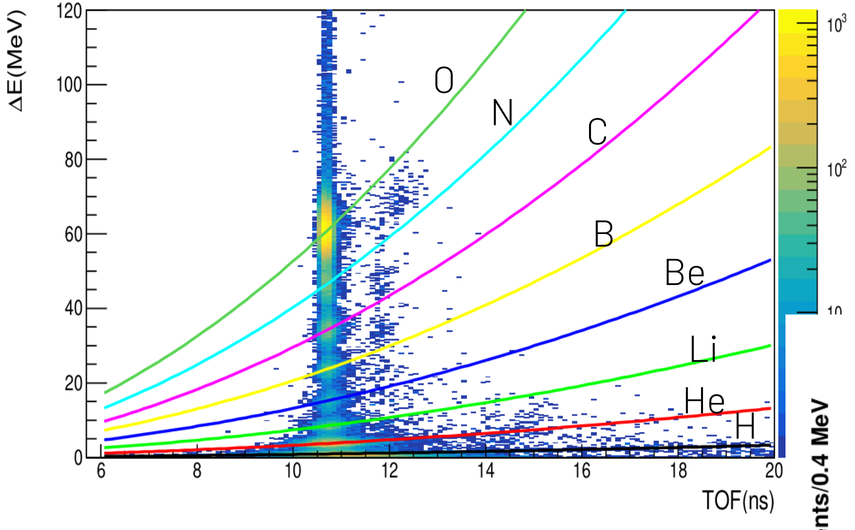

400 MeV/u ^{16}O beam on 5mm Carbon target

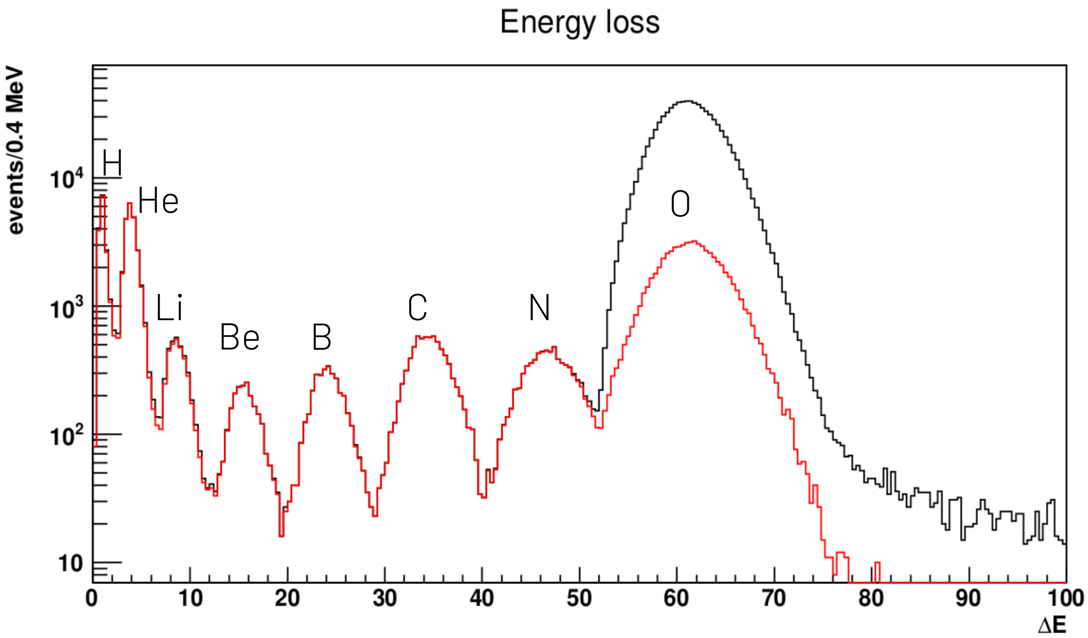

excellent charge separation!

Cross sections

400 MeV/u ^{16}O beam on 5mm Carbon target

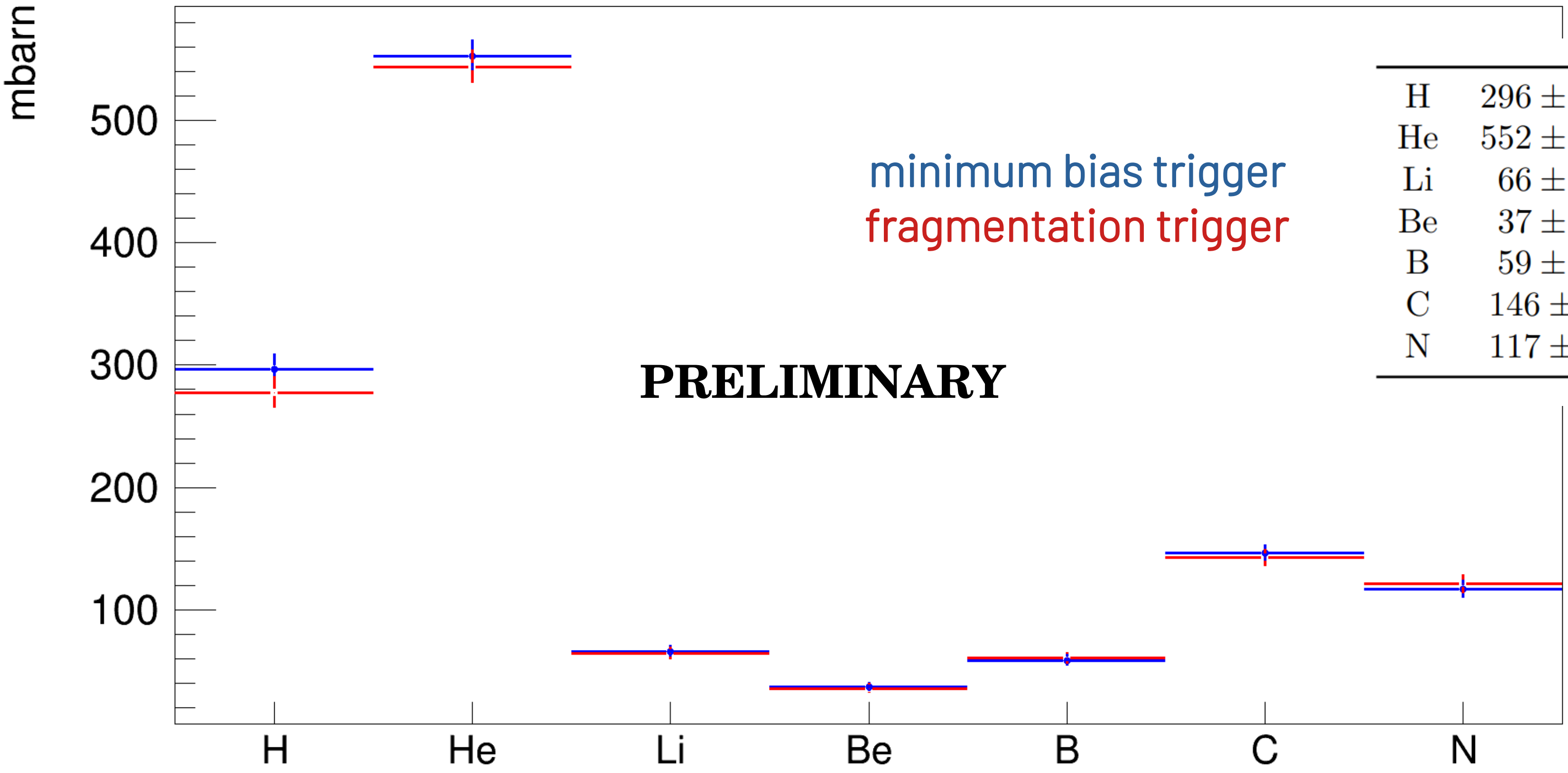

H	296 ± 13 mb
He	552 ± 13 mb
Li	66 ± 5 mb
Be	37 ± 4 mb
B	59 ± 5 mb
C	146 ± 7 mb
N	117 ± 8 mb

Cross sections

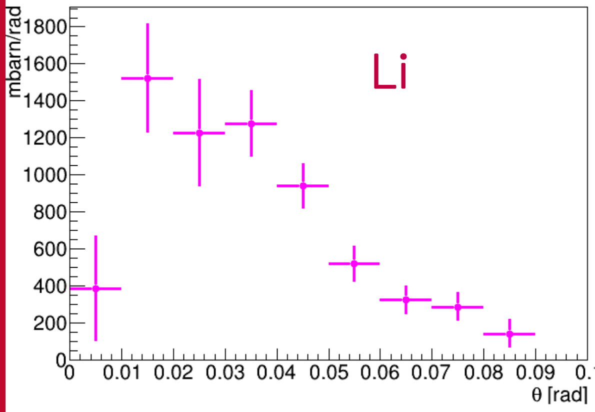

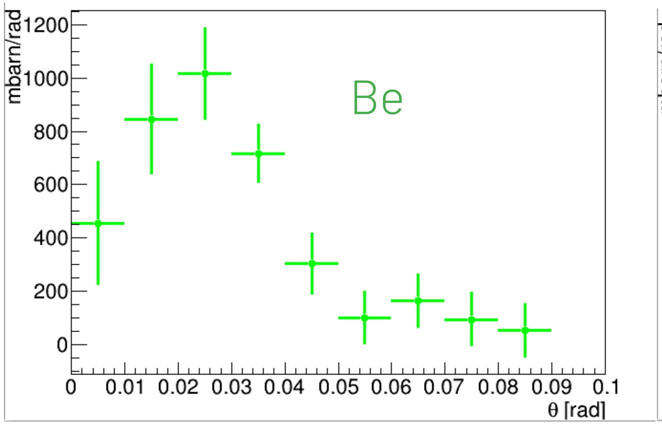

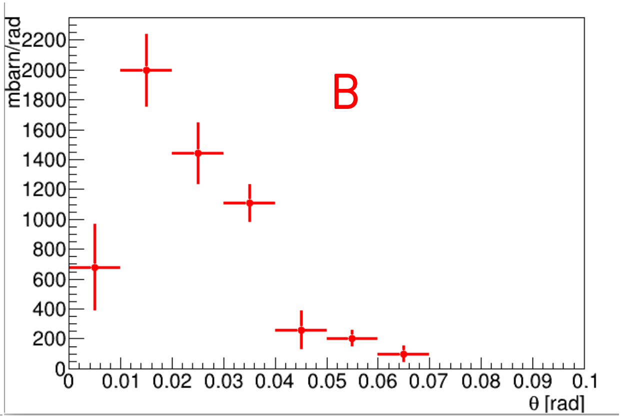

PRELIMINARY

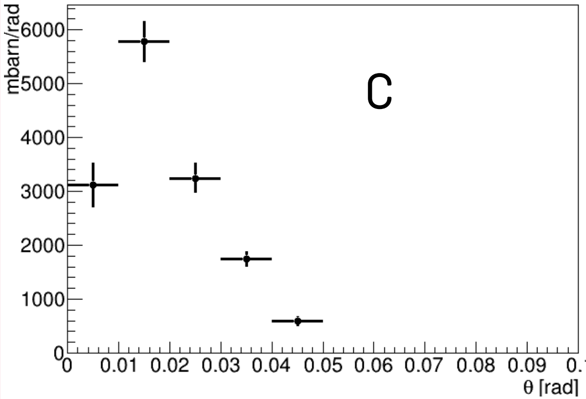

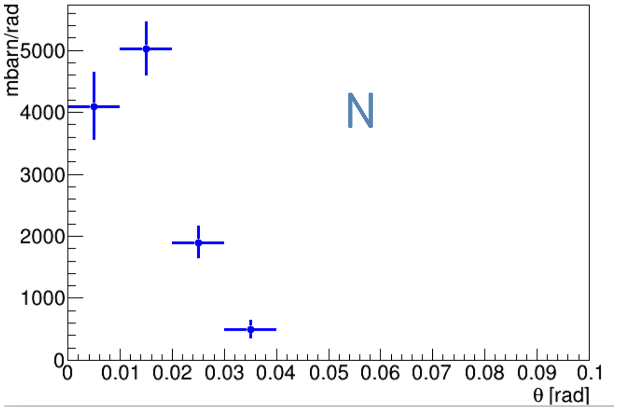

First available measurements!

Activities in Bologna

Trigger and Data Acquisition (TDAQ)

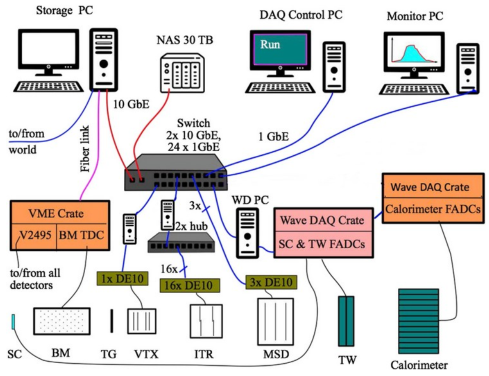

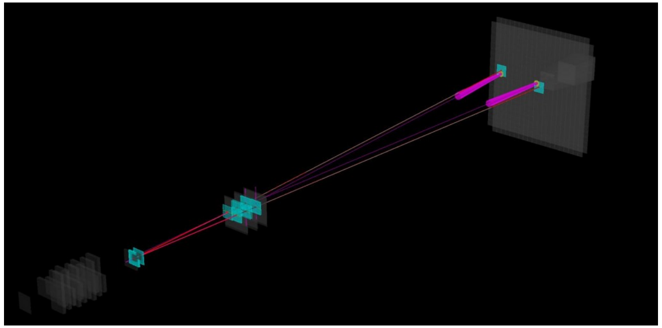

Global tracking

Data analysis

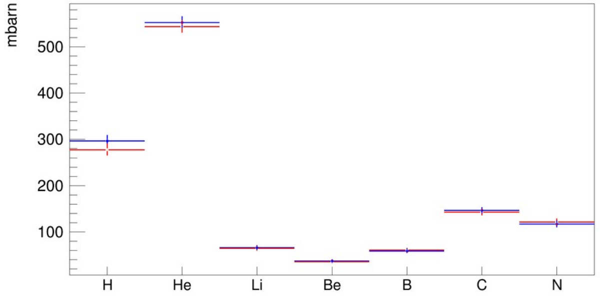

Thanks for listening!

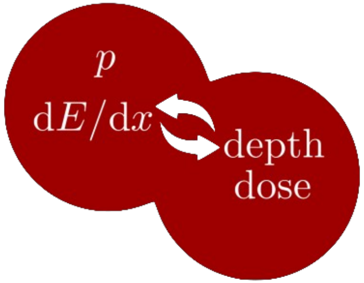

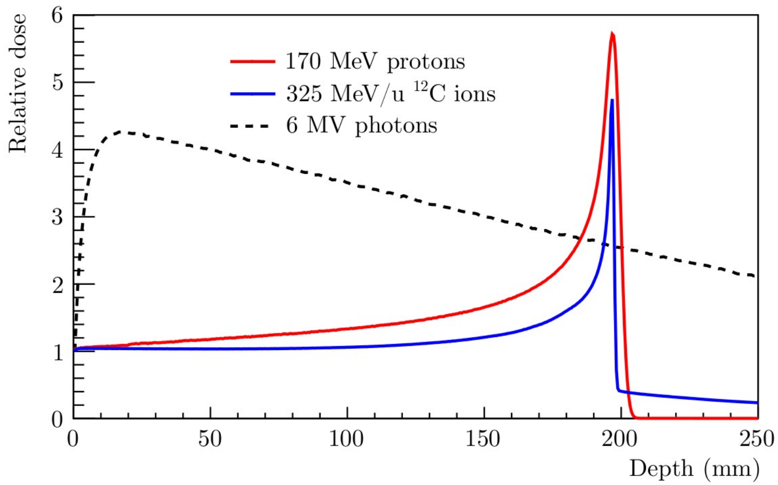

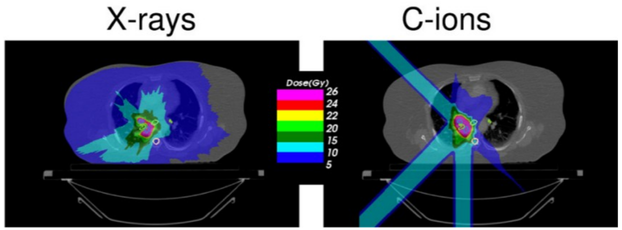

$$-\left\langle \frac{\mathrm{d}E}{\mathrm{d}x} \right\rangle = \frac{2\pi N_a e^4 \rho}{m_e} \frac{Z}{A} \frac{z^2}{v^2} \left[\ln \left(\frac{2 m_e \gamma^2 v^2 W_{\max}}{I^2} \right) - 2\beta^2 - \delta - 2\frac{C}{Z} \right]$$

$$p = \frac{\sqrt{E_k\left(E_k + 2m_0c^2\right)}}{c} \qquad \mathcal{E} = \frac{E_k}{m_0c^2}. \qquad \beta\gamma = \sqrt{\mathcal{E}(\mathcal{E}+2)}.$$

$$R_{m_x} \approx \frac{m_x}{m_p}\frac{z_p^2}{z_x^2} R_{m_p} \qquad \frac{\sigma_{R1}}{\sigma_{R2}} \approx \sqrt{\frac{m_2}{m_1}}.$$

$$\sigma_R = \pi r_0^2 c_1(E) \left(A_p^{1/3} + A_t^{1/3} - c_2(E) \right)^2$$

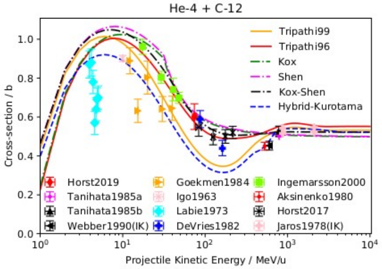

(a)

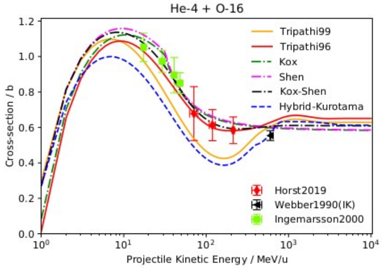

(b)

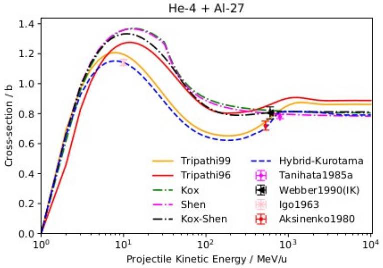

(c)

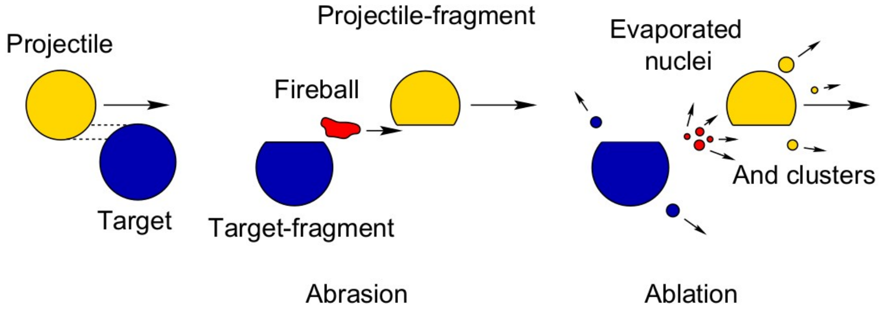

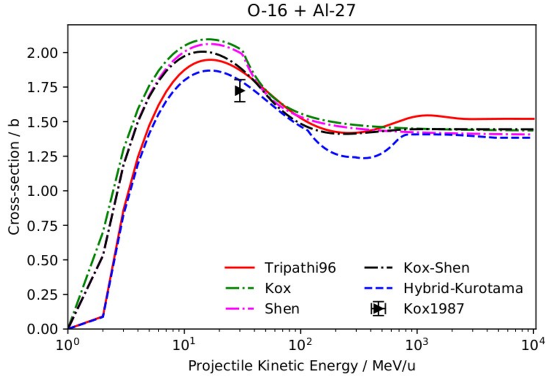

Comparison with literature

PHYSICAL REVIEW C **83**, 034909 (2011)

Fragmentation of ^{14}N, ^{16}O, ^{20}Ne, and ^{24}Mg nuclei at 290 to 1000 MeV/nucleon

C. Zeitlin*
Southwest Research Institute, Boulder, Colorado 80302, USA

J. Miller
Lawrence Berkeley National Laboratory, 1 Cyclotron Road, Berkeley, California 94720, USA

S. Guetersloh
Department of Nuclear Engineering, Texas A&M University, College Station, Texas 77843, USA

L. Heilbronn
Department of Nuclear Engineering, University of Tennessee, Knoxville, Tennessee 37996, USA

A. Fukumura, Y. Iwata, and T. Murakami
National Institute of Radiological Sciences, Chiba, Japan

S. Blattnig and R. Norman
NASA Langley Research Center, Hampton, Virginia 23681, USA

S. Mashnik
Los Alamos National Laboratory, Los Alamos, New Mexico 87545, USA
(Received 27 October 2010; revised manuscript received 20 January 2011; published 24 March 2011)
10.1103/PhysRevC.83.034909

We report fragmentation cross sections measured at 0° for beams of ^{14}N, ^{16}O, ^{20}Ne, and ^{24}Mg ions, at energies ranging from 290 MeV/nucleon to 1000 MeV/nucleon. Beams were incident on targets of C, CH_2, Al, Cu, Sn, and Pb, with the C and CH_2 target data used to obtain hydrogen-target cross sections. Using methods established in earlier work, cross sections obtained with both large-acceptance and small-acceptance detectors are extracted from the data and, when necessary, corrected for acceptance effects. The large-acceptance data yield cross sections for fragments with charges approximately half of the beam charge and above, with minimal corrections. Cross sections for lighter fragments are obtained from small-acceptance spectra, with more significant, model-dependent corrections that account for the fragment angular distributions. Results for both charge-changing and fragment production cross sections are compared to the predictions of the Los Alamos version of the quark gluon string model (LAQGSM) as well as the NASA Nuclear Fragmentation (NUCFRG2) model and the Particle and Heavy Ion Transport System (PHITS) model. For all beams and targets, cross sections for fragments as light as He are compared to the models. Estimates of multiplicity-weighted helium production cross sections are obtained from the data and compared to PHITS and LAQGSM predictions. Summary statistics show that the level of agreement between data and predictions is slightly better for PHITS than for either NUCFRG2 or LAQGSM.

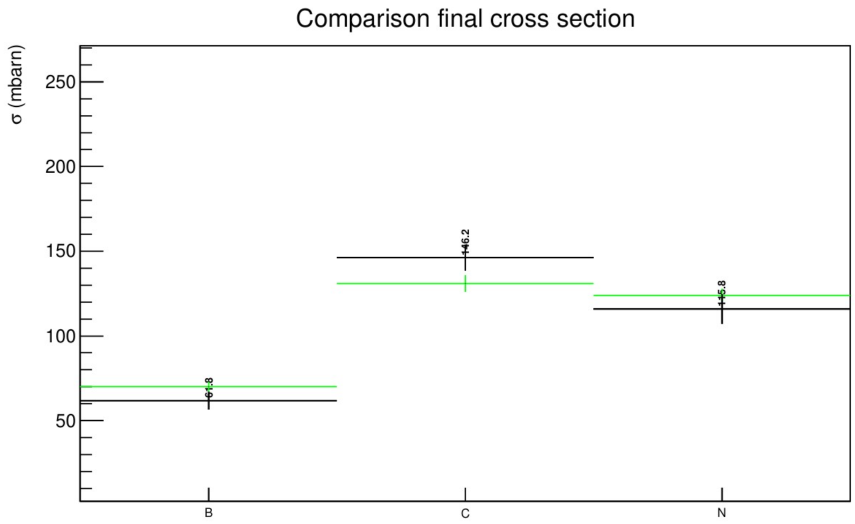

	This work	Ref.[69]	Weighted average	t
B	62 ± 5	70 ± 3	68.0 ± 2.6	-1.37
C	146 ± 8	131 ± 5	135.5 ± 4.2	1.66
N	116 ± 9	124 ± 4	122.6 ± 3.6	-0.86

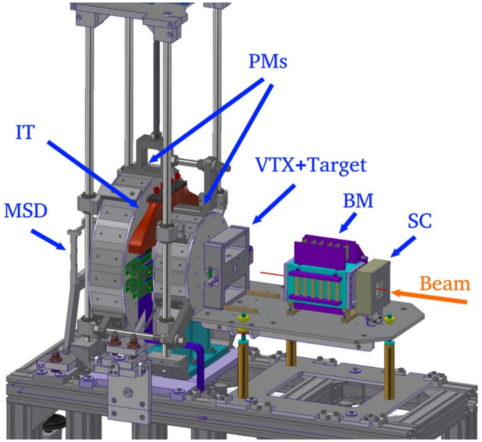

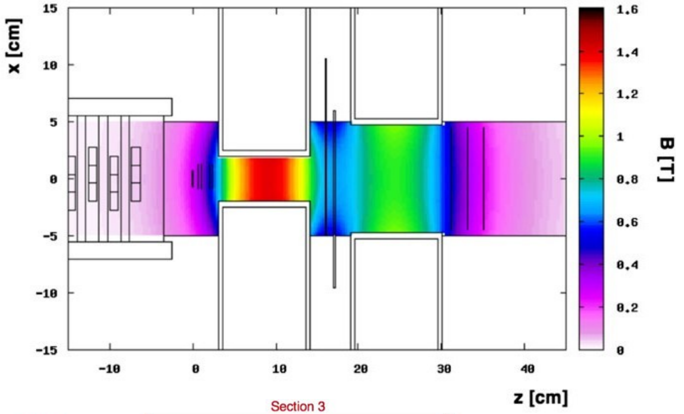

$$p = mc\beta\gamma$$

$$E_{\text{kin}} = mc^2(\gamma - 1)$$

$$E_{\text{kin}} = \sqrt{p^2c^2 + m^2c^4} - mc^2$$

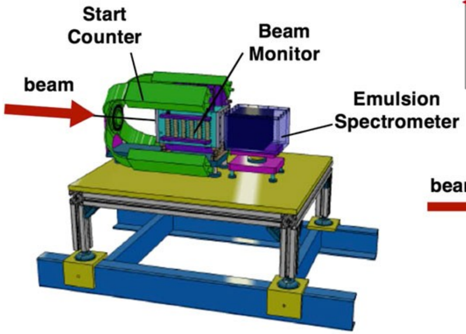

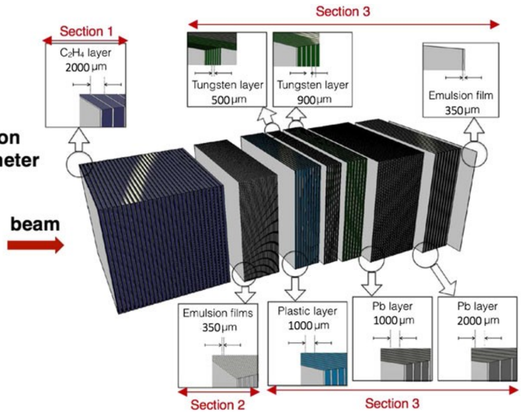

- $\sigma(p)/p$ at level of 4 – 5%;
- $\sigma(T_{\text{tof}})$ at level of 100 ps;
- $\sigma(E_{\text{kin}})/E_{\text{kin}}$ at level of 1 – 2%;
- $\sigma(\Delta E)/\Delta E$ at level of 5%;

Emulsion setup: first results

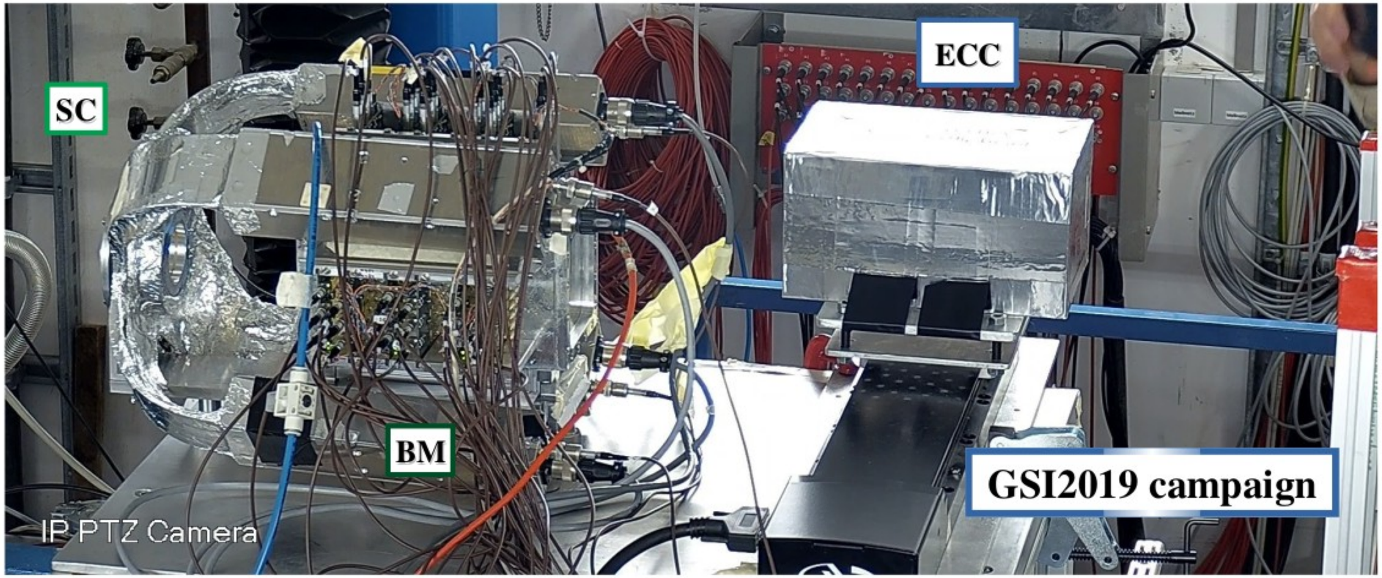

- Data acquisitions started in 2019
- SC + BM for primary beam monitoring
- Only charge identification up to now

$^{16}O + C/C_2H_4$ @ 200 MeV/u

Emulsion setup: first results

Charge identification in Section2:

- Different thermal treatment for track etching
- Cosmic rays cut-based rejection
- Principal Component Analysis for Z ≥ 1

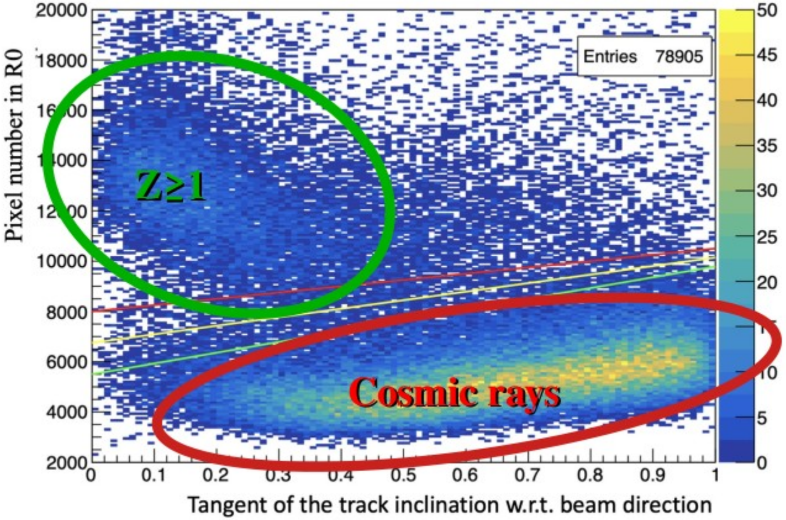

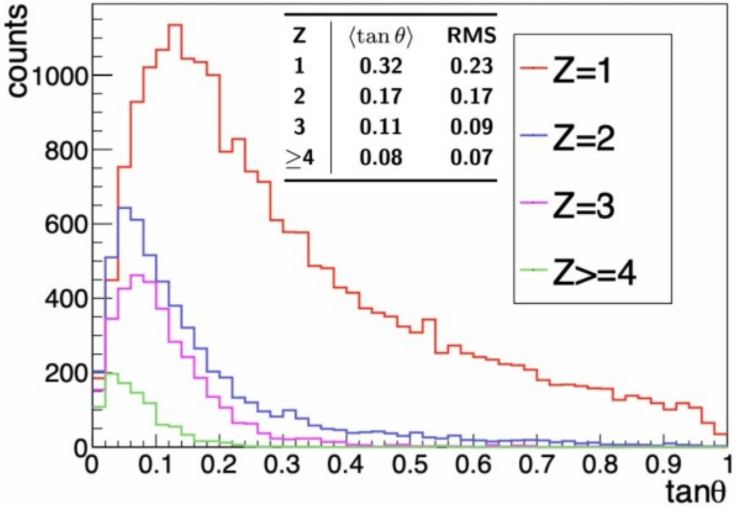

Z	⟨tan θ⟩	RMS
1	0.32	0.23
2	0.17	0.17
3	0.11	0.09
≥4	0.08	0.07

^{16}O + C/C_2H_4 @ 200 MeV/u

Emulsion setup: first results

PRELIMINARY

$$\left.\frac{d\sigma(\theta)}{d\theta}\right|_{C\ or\ C_2H_4} = \frac{Y_i(\theta)}{N_B N_{TG} \Delta\theta \epsilon^i_{reco}(\theta)}$$

^{16}O (200 MeV/u) + C/C_2H_4

Differential Cross Sections

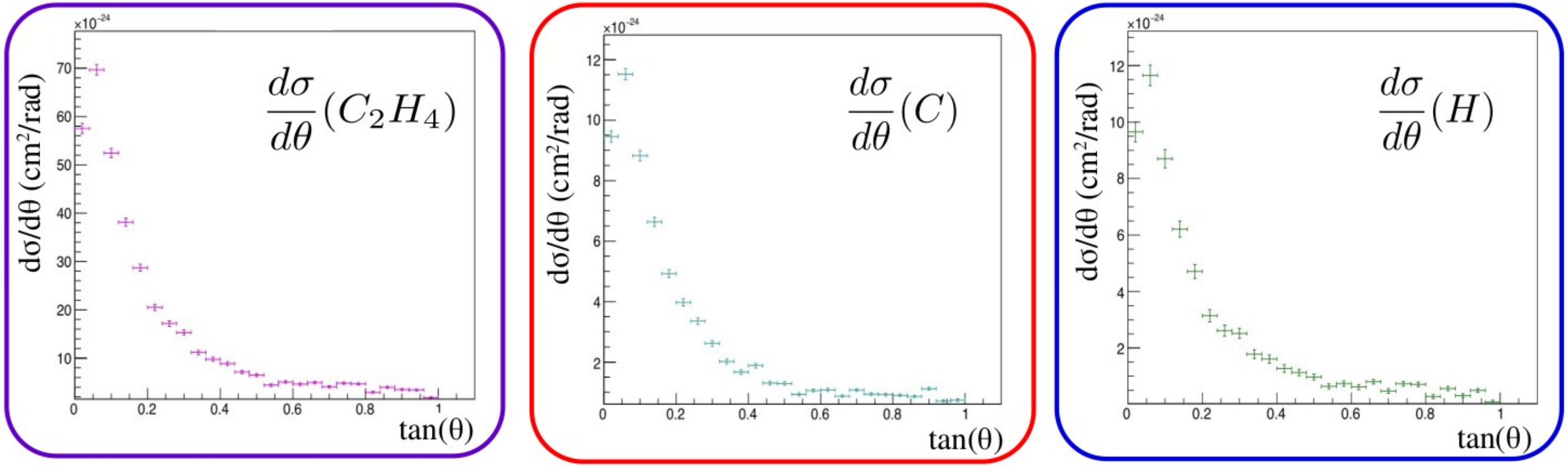

Courtesy of G. Galati

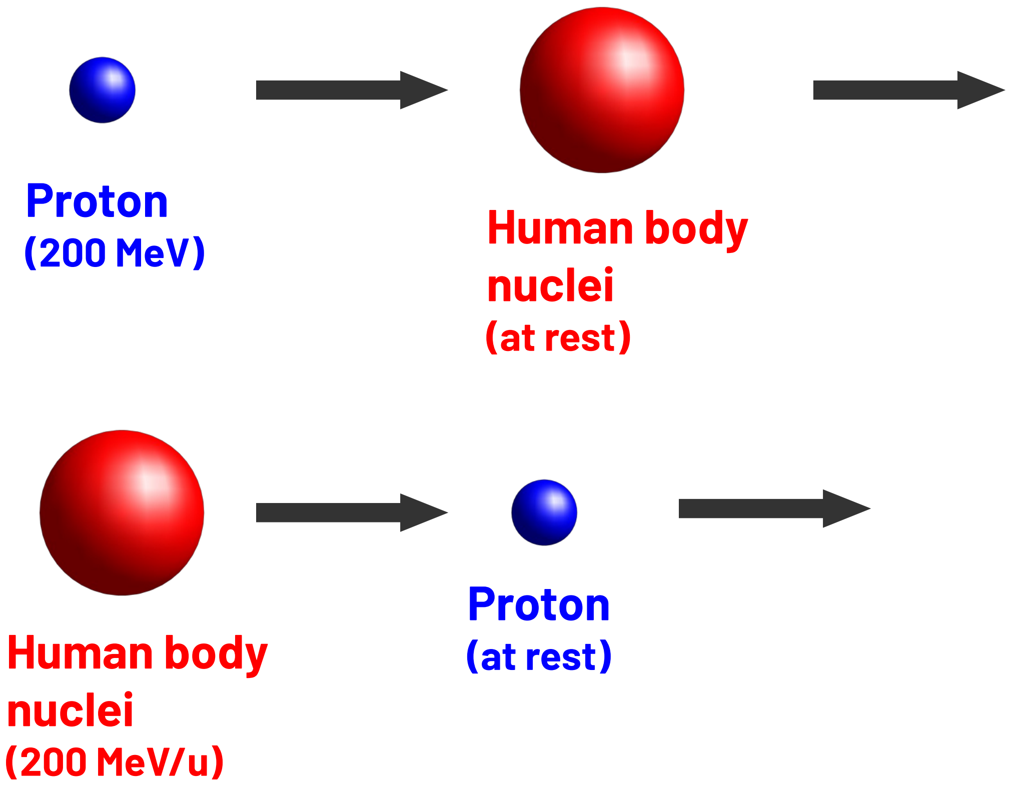

Fragments with low energy and short range (few cell diametres) ✗

Very difficult to detect!

Fragments with higher energy and longer range! ✓

Problem: hydrogen target

- ✗ gas is not allowed in all experimental rooms
- ✗ gas is too sparse (low interaction probability)

Polyethylene target $(C_2H_4)_n$ and Carbon target

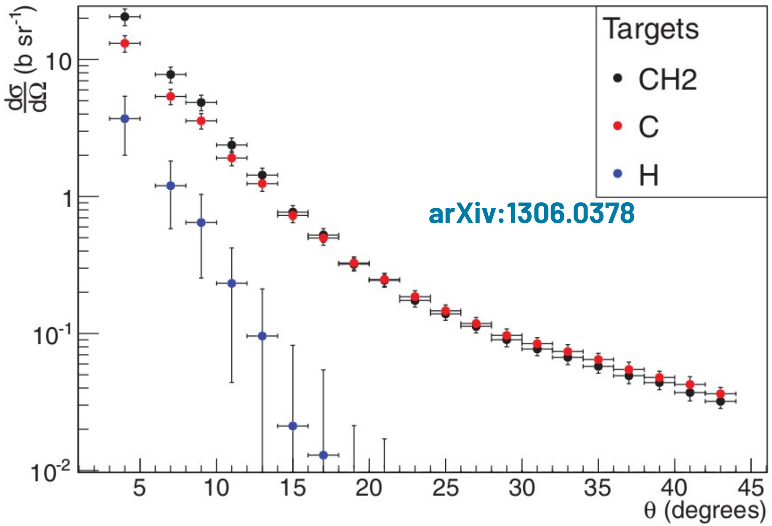

$$\frac{d\sigma}{d\Omega}(H) = \frac{1}{4} \cdot \left(\frac{d\sigma}{d\Omega}(\mathrm{C_2H_4}) - 2 \cdot \frac{d\sigma}{d\Omega}(\mathrm{C}) \right)$$

TDAQ infrastructure

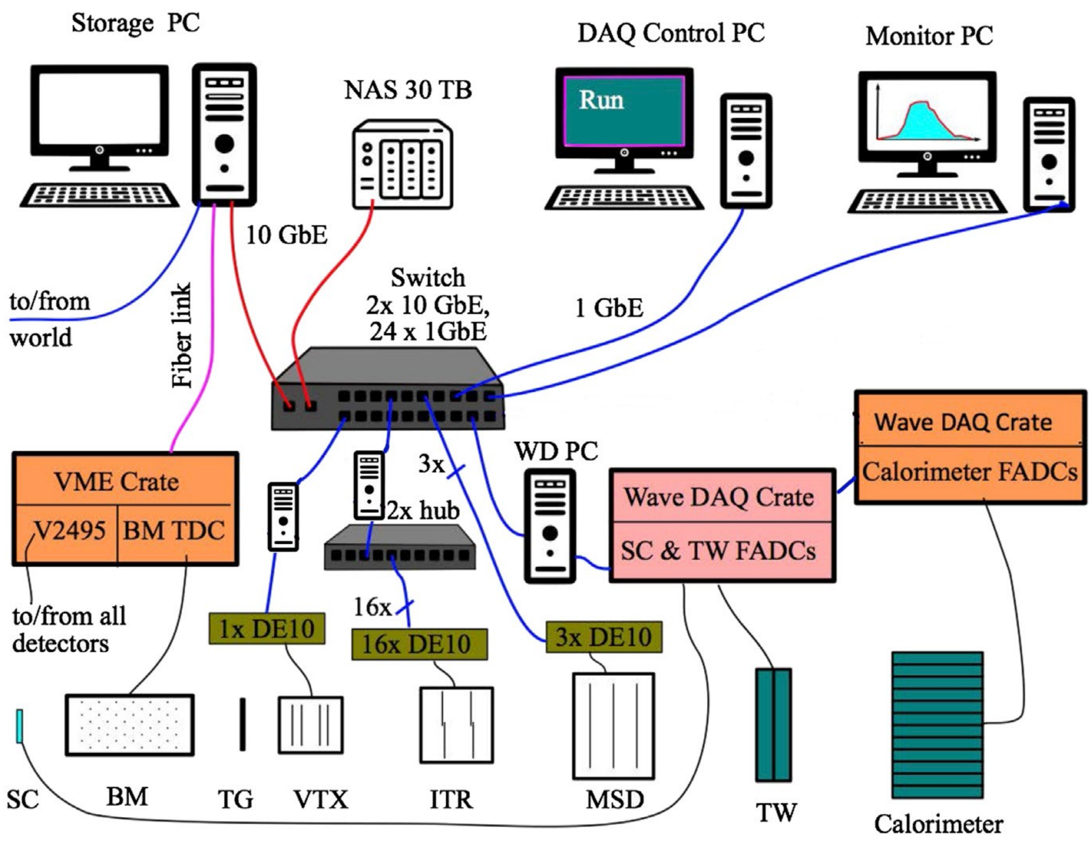

-**flexible and distributed** system
VME, Linux PC, custom boards, Ethernet, optical fibers
-**70 kB/event**
1 kHz acquisition rate
2 TB/day
-V2495 handles **trigger and busy signals**
-data path is not signal path